Detection of Eyebolt Faults Using a Random Forest Ensemble Model Based on Multiple High-Frequency Electromagnetic Parameters

H. V. H. Silva Filho [1*] , R.G. M. dos Santos [1] , Douglas C. P. Barbosa[1] , M. T. de Melo[1] , Lauro R. G. S. Lourenço Novo[1]

[1]Federal University of Pernambuco, Recife, Brazil

Abstract—**This paper presents an eyebolt structural fault detection system, based on the analysis of multiple electromagnetic parameters through a random forest classifier trained by both measurements and high-fidelity simulated signals. The proposed methodology is completely noninvasive and does not require the disassembly of the electrical infrastructure, allowing the live-line working. The obtained results show that the proposed multi-parameter strategy achieves high accuracy and increases the system's capability of detecting faults, improving the efficiency of the operator's preventive maintenance routines and, consequently, increasing the reliability of the power supply and energy distribution systems.**

Index Terms— Anchoring eye bolts, fault detection, random forest algorithm and transmission lines.

I. INTRODUCTION

Concrete columns and beams are widely used to support aerial electrical cables in voltage classes below 69 kV for power transmission lines (TL) and 230 kV for substations (SEs). In such applications, anchoring eye bolts are typically used to fix the electric power cables to high voltage insulators on poles and towers. Fig. 1 (a) and Fig.1 (b) shows typical applications of eye bolts in aerial cable anchorage for both an urban 69 kV transmission line and Fig.1 (c) show 230 kV substation.

Over time, the effects of the weather, friction, and mechanical stress cause the eye bolts to lose their desired physical characteristics. The bolt structure can undergo corrosion processes that lead to the degradation of the metallic material, causing the weakening of mechanical properties such as strength, elasticity, and ductility, as shown in Fig. 2 [1]-[3]. Corrosion and wear of such elements are problems that put the electricity supply at risk and expose the operators of the transmission and distribution lines to financial penalties and sanctions by regulatory agencies in the event of any accident.

The good appearance of the visible part of the eye bolt's structure does not guarantee the integrity of the respective embedded parts inserted into the bodies of concrete. Additionally, the lack of inspection of the eye bolts of TLs and SEs can cause major accidents. For this reason, electrical companies must maintain constant monitoring of the degradation state of such elements, which has traditionally been done through visual inspection.
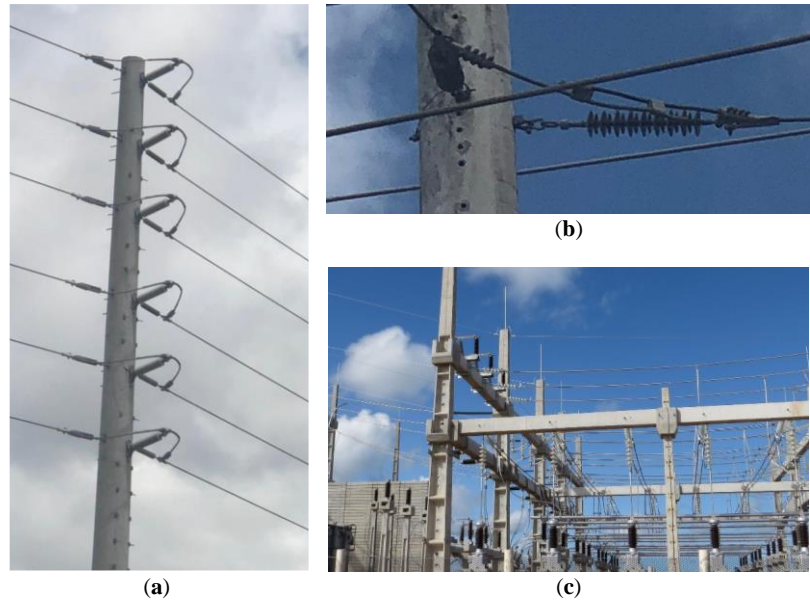
Fig.1. Applications of eye bolts. a) Dual transmission lines 69 kV; b) Anchoring of insulator chains 69 kV and c) Bay substation 230kV.

Fig. 2. Effect of corrosive process in eye bolts

Fig. 3 shows the detailed view of the typical assembly scheme for the cable anchoring system using eye bolts. In maintenance routines, the visible parts of the eye bolts are relatively easy to inspect with the naked eye. However, the examination of the embedded parts of the eye bolts that are out of visual reach requires a different approach. In the traditional maintenance procedure, for the complete visual inspection of the eye bolts embedded into concrete beams or posts, the entire disassembly of the anchoring structure is necessary.

The disassembly of a power line or bus will imply either the laying of cables on the ground or the installation of a temporary anchorage to guarantee the safe release of the inspected anchorage elements during the assessment of the structure. Such a process implies the temporary electrical disconnection of the substation transmission line or bus for a considerable time, representing a major operational inconvenience which entails the increase in direct costs and contractual supply charges to the electrical companies.
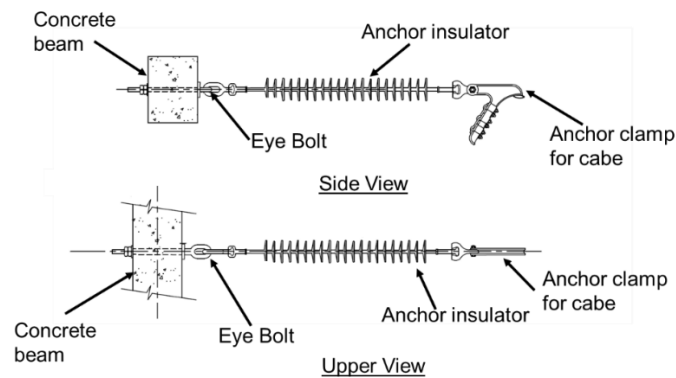
Fig. 3. Typical 69 kV eye bolt anchoring scheme.

Due to this problem, the goal of this work is to propose a fault detection methodology in eyebolts with no necessity of disassembling the anchorage of the electrical insulators. This is based on a random forest classifier in the analysis of multiple electromagnetic parameters [4], [5].Enabling the verification of the presence or absence of faults in the eyes without the need to turn off or interrupt the power supply, obtaining a reduction in costs and maintenance time, which improves the performance of operation and maintenance (O&M) procedures, as problems arise downtime can cost around 1 to 2% of the responsible company's annual turnover [6], [7]. Thus, this methodology increases the reliability of the anchoring, as well as the availability and safety of the electrical system.

II. RELATED WORKS

Approaches of fault detection are abundant in literature for different types of embedded or hidden metallic structures. In [8] a ground rod corrosion detection technique is presented. Applications of discontinuity detection in coaxial cables are found in [9] and [10] using frequency-domain reflectometry and in [11] using time-domain reflectometry. In [1] is presented an application of microwaves for the characterization of steel corrosion stages. In [13] an application of an RFID sensor for monitoring corrosion of steel in concrete using the reflection parameter S11 is presented. In [14], is presented an investigation of the low-frequency stray current induced corrosion on reinforced concrete infrastructure in high-speed electrified rails.

Several approaches for detecting, classifying, and locating faults in metallic structures used to support cables of power transmission systems have already been proposed. In [4], [5], [15] and [16], the analysis of microwave signals of anchor rods using frequency-domain reflectometry is discussed. In [17], a model based on PSO-SVM is proposed to detect faults in anchor rods of guyed towers of power transmission lines. The approach presented in [18] provides an anchor bolt fault classification based on spectral kurtosis and K-means clustering algorithm. On the other hand, machine learning tools are naturally able to learn the underlying relationships between the inputs and the outputs of a given system and automatically extract features capable of differentiating patterns. Such feature extraction allows the machine learning model to perform generalization from the knowledge acquired from a restricted set of

examples and to predict future situations with a high degree of accuracy [26], [27].

In [21], a system for detecting corrosion in grounding systems is presented. In [22], a technique based on neural networks for detecting corrosion in industrial pipes is proposed. In [23], is discussed a technique for corrosion detection of metallic structures and substations based on deep learning. In [24], a machine learning model is presented to locate faults in underground anchor rods through the analysis of the input impedance signals. In [25], an edge intelligent recognition method based on a deep neural network is proposed to detect faults on transmission line insulators.

In [4], [5] and [16], there are similar applications for fault detection in anchor rods used in guyed towers for electric power transmission. In [4], a comparison of different ML classification algorithms (Logistic Regression, K-NNs Random Forest, SVM and ANN) is presented in the task of detecting structural failures in anchor rods, in order to define the most suitable one for this task. For This application, the Random Forest was the algorithm with the best results. In [5], an analysis of multiple electromagnetic parameters was presented using artificial neural networks as a binary classifier for detection of failures in anchor rods. It was identified that the use of a classifier (ensemble) for the association of parameters ($|S11|$, Phase{S11}, VSWR, $| Z_{in} |$}, obtained a higher accuracy when compared to the individual results. In [16] he presented a field application system for detecting structural failures in anchor rods of guyed towers of power transmission lines, based on reflectometry in the frequency domain. A machine learning framework was developed for the signals of parameter $|S11|$ measurements of different buried rods to classify them as normal or defective.

In [19] and [20] techniques are presented to measure microwave signals of eye bolts. In [20] he presented an approach aimed at the design of the eyelet adapter and the study of the sensitivity of this adapter for six types of samples applied to a simplified system. Concrete was not used as a dielectric medium, but air, and did not present any system classification. In [19], a more complete approach was presented than the one presented in [20] for detecting structural failures in eye bolts, a system was proposed considering the presence of concrete as a dielectric medium and an intelligent system based on an artificial neural network to process the measured reflectometry signals for the presence or absence of wear on eyebolts.

Based on [4], [5] and [19], this work presents a more accurate solution to the problem of detecting structural failures in anchoring eyes for power transmission lines. Because the random forest algorithm was used, which offers a greater capacity for data interpretation, is less susceptible to overfitting and outliers compared to the Artificial Neural Networks presented in [19], according to [4]. This article also proposes a method to evaluate the performance of a machine learning model using the k-fold cross-validation technique [4] and in addition to accuracy, precision, recall and f1-score were analyzed to measure the performance of the system. Proposed, unlike [19], presented a more simplified system without taking into account performance systems for validating the results. A broader database with different analysis signals is also presented, making it possible to compensate for any mistakes made when compared to systems. This way, there is only one signal under analysis when compared to the

system presented by [19]. In addition, it is important to highlight that there is a significant difference between the anchor rod and the eye bolt, where the screws have a length and a smaller diameter than the anchor rod, so the connector presented in this article is different from those presented by [4], [5] and [16].

Thus, the main contribution of this work is to present a more reliable and viable technique to evaluate the structural condition of the eyes without the need to dismantle the anchoring system as is traditionally done, allowing the early detection of structural failures in such elements with a high accuracy. Based on a random forest classifier in the analysis of multiple input parameters, it provides the detection algorithm with a diversity of representations of the structure under analysis, which increases the detection performance of the system, when compared to systems with only one input parameter. Table I presents a comparison of the general characteristics of systems similar to the proposed one.

Table I. General characteristics of similar fault detecting systems.

Ref	Structure	Objective	Signal	Parameter	ML Algorithm
[4]	Anchor rod	Fault Detection	Microwave	$\|S11\|$	Logistic Regression K-NNs Random Forest SVM ANN
[5]	Anchor rod	Fault Detection	Microwave	S11 VSWR Input Impedance	ANN
[8]	Ground rod	Corrosion detection	Longitudinal acoustic guided waves	Pulse-echo	None
[9]	Coaxial cable	Fault location	Microwave	Impedance in the frequency domain	None
[10]	Coaxial cable	Fault location	Microwave	Impedance Spectroscopy	None
[11]	Steel cable	Fault location	Microwave	Γ (Reflection coefficient)	None
[12]	Steel in Concrete	Characterization of steel corrosion stages	Microwave	$\|S11\|$	None
[13]	Steel in concrete	Corrosion detection	UHF	$\|S11\|$	None
[15]	Anchor rod	Fault Detection	Microwave	$\|S11\|$	None
[16]	Anchor rod	Fault Detection	Microwave	$\|S11\|$	Logistic Regression
[17]	Anchor rod	Fault Detection	Vibration	Signal characteristics (mean value, peak value, peak-to-peak value, standard deviation, kurtosis, root mean square value, etc.)	PSO-SVM
[19]	Eye bolt	Fault Detection	Microwave	$\|S11\|$	ANN
[20]	Eye bolt	Fault Detection	Microwave	$\|S11\|$	None
Proposed System	Eye bolt	Fault Detection	Microwave	S11 VSWR Input Impedance	Random Forest

III. METHODOLOGY

To approach a transmission line, a low-loss device was designed connecting the eye bolt, the reference bar and the VNA voltage source. Such a device, called eyelet adapter [20], allows applying a high frequency wave to the system, measuring a respective reflected one, and thus obtaining a set of electromagnetic parameters of the presented transmission line [30]. Such parameters are altered by discontinuities in the medium in which the wave propagates and, therefore, carry information about the presence of possible failures in the eye bolt structure [13], [31]. As the eye bolt is essentially a metallic conducting cylinder, it is possible to couple along it a parallel conductor called the reference rod, so that the system behaves as a transmission Line. Once such approach has been established between the conductors, the evaluation of the electromagnetic parameters of the structure is made possible by connecting the N connector port to a Vector Network Analyzer (VNA) [28], [29], as shown in Fig. 4.
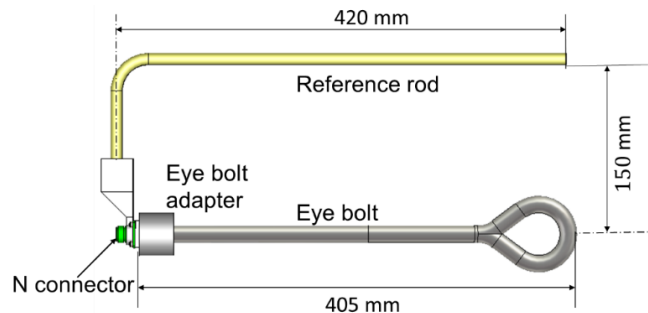

Fig. 4. Setup of the TL formed by the eye bolt and the reference rod.

The operating principle of the proposed measurement system is based on the transmission lines theory and multiple reflections for media with different impedances [1], as presented in Fig. 5. An incident electromagnetic wave that propagates in a physical medium, upon encountering an interface with another one of different characteristic impedance, undergoes reflection and refraction. The proportion between how much of the wave is reflected and how much is refracted depends on the specific characteristics of both media and is given by the reflection coefficient Γ.
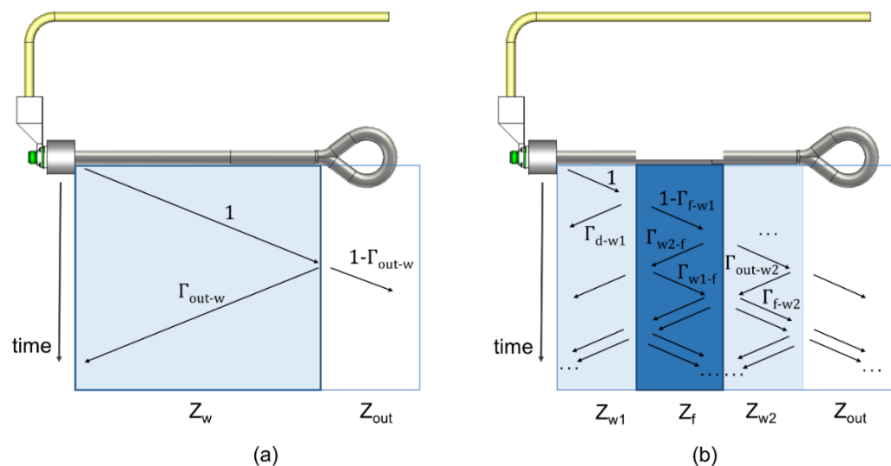

Fig. 5. Operating principle of the proposed multiple reflections detection system. (a) faultless bolt. (b) faulty bolt.

Where, Z_w represents the characteristic impedance of the eye bolt, Z_{out} the medium change impedance, Z_f the fault impedance. Z_{w1} and Z_{w2} are the characteristic impedances of the bolt of the sections before and after failure, even though they are made of the same physical material, they are represented by different impedances because, due to the geometric changes caused by the failure, they may behave as different electromagnetic media.

Thus, as there are different patterns of interaction between the incident and reflected waves that propagate in the eyebolt for cases with and without failures. The detection can be performed by analyzing the characteristics of the reflected signals extracted from high frequency and VNA parameters, such as loss of feedback |S11|, Phase{S11}, input impedance (Z_{in}) and voltage-wave ratio (VSWR). Even the parameters are highly correlated and can even be mathematically derived from one another. However, from the point of view of the machine learning model, they are different representations of the same measure. Generally, as more diverse representations of the observations are available to feed the machine learning algorithm (in this specific case, a random forest), more information can be extracted from the data by the model, allowing for better results. This fact can be observed when the model simultaneously processes the data of all five analyzed EM parameters and the measured performance (for example, Precision, F1-Score, Rec, Prec) is superior, when compared to those obtained for each of the five EM parameters, if analyzed individually [5]. This approach is possible due to the low computational processing time of the random forest model developed for the chosen EM parameter data.

A. Eye adapter design and EM simulation for database generation

Initially, the system setup was modeled using an electromagnetic simulation program, Ansys HFSS 2019 [32] to obtain the correct dimensions of the connecting devices and ensure the electromagnetic coupling between the eye bolt and a 50 Ω-port VNA.

The eye adapter has a cylindrical shape in aluminum, so that, only the central pin of the female N connector has electrical contact with the eye bolt through the adapter's cylindrical surface. For this reason, a Teflon part and bushings have been designed to isolate it from the external part of the N connector. The reference rod is characterized by a Ø 3/8 " cylindrical bar with a SAE 1020 carbon steel core covered with a thin copper layer electrolytic, and 420 mm of length in parallel with the bolt. The eye adapter mechanically connects and electromagnetically couples the eye bolt and the reference rod, keeping 150 mm of separation between the conductors. The general view of the set-up, including the concrete block, the typical mounting accessories, and the details of the adapter are shown in Fig. 6.
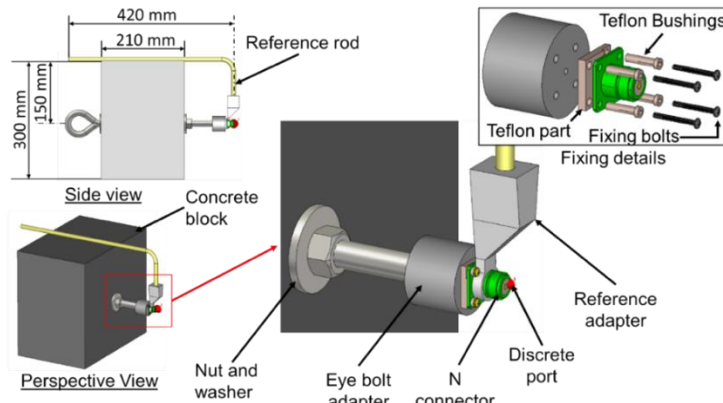
Fig. 6. Simulation setup.

A database with 1430 simulated samples was built to provide to the machine learning model a source of signals corresponding to different types of failures. As shown in Fig. 7, in addition to the faultless bolt, on each simulation, the length (LE), depth (DE) and distance of the fault to the connection point (DI) are varied, in the range presented in Table II.
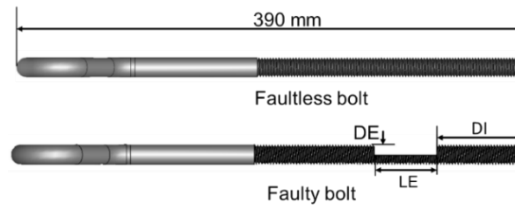

Fig. 7. Details of the eyebolt simulation model for the faultless and faulty setups.

Table II. Dimensions of the fault parameters on the simulated bolts.

Parameter	Dimensions (mm)
Length (LE)	5, 25, 50, 75, and 100
Depth (DE)	0.1 to 8.0 with step 0.1
	9, 10, 11, 12, and 13
Distance (DI)	75, 100, 125, 150, 175, 200 and 225

B. Measurement system

To perform the measurements with safety, a concrete block with the approximate dimensions of the beams and columns commonly found in 230 kV and 69 kV substations as well as in 69 kV transmission lines was used to emulate the concrete structures in which the eye bolts are inserted.

The measurement arrangement has also considered a portable vector network analyzer (FieldFox 9952A), a concrete block, nuts, washers, the eye bolt adapter, and the bolts, as shown in Fig. 8. The concrete block used in the measurements has the same dimensions as the one used in the simulations performed.
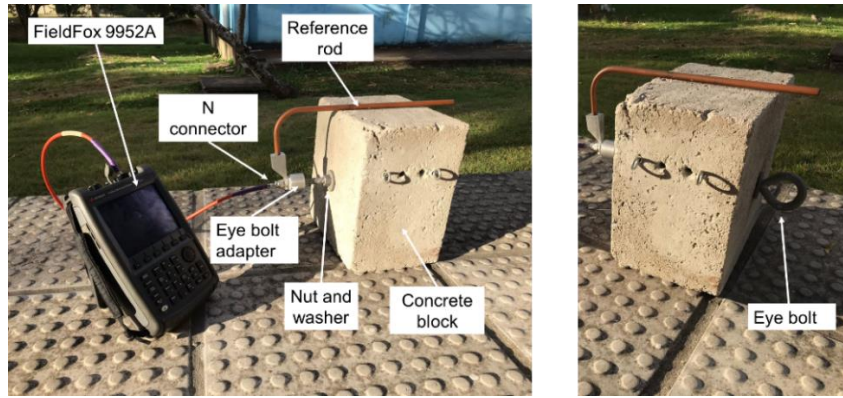
Fig. 8. Measurement setup.

For the measurement model, hot-dip galvanized steel eye bolts (AISI / SEA 1045) with a diameter of 15.87 mm (5/8") and a length of 390 mm were used. The reference rod was built with a central carbon steel rod with an electrolytic sheath (SAE 1010/1020) with a diameter of 9.52 mm (3/8") and a parallel length of 420 mm. A set of 7 distinct eyebolt samples have been prepared for measurements, as shown in Fig. 9, which dimensions of the interest parameters are presented in Table III.

Fig. 9. Configurations of the measured bolts: a) Side view b) Top view

Table III. Dimensions of the fault parameters of the measured bolts.

Bolt	Length (LE) (mm)	Depth (DE) (mm)	Distance (DI) (mm)
B0	Faultless sample		
B1	50	8	70
B2	25	8	110
B3	50	2	110
B4	50	8	110
B5	100	8	110
B6	50	8	250

Each bolt sample was measured several times in a series of data acquisitions so that the signal variations such as inherent errors related to the measurement process, bad connections, and noise were eliminated by the classifier. A total of 580 measurements were performed with the 7 bolt samples. They were divided into 220 measurements of the normal bolt and 60 for each one of the 6 faulty bolt samples. The same frequency range and resolution points used in the simulations were adopted in the

measurements to ensure the full compatibility between the data acquired on both setups.

IV. BINARY CLASSIFICATION BASED ON RANDOM FOREST ALGORITHM

Samples obtained from the m eye bolts are organized in a parameter matrix $X_{m\ x\ n}$, where each line $x_i = \left(x_{i1}^1, x_{i2}^1, \dots, x_{in}^1\right)|\left(x_{i1}^2, x_{i2}^2, \dots, x_{in}^2\right)| \dots |\left(x_{i1}^5, x_{i2}^5, \dots, x_{in}^5\right)$ contains an input vector composed by the concatenation of data referring to the following EM parameters: magnitude of S11, phase of S11, the real part of Z_{in}, the imaginary part of Z_{in}, and VSWR (Voltage Standing Wave Ratio), referring to the ith bolt. Each EM parameter is sampled at equally spaced n = 501 points in a frequency range from 200 to 600 MHz for both simulation and measurement data. This frequency range was chosen because it allows the observation of at least one point of resonance, has a low frequency shift between the measured and simulated signals and the development of a both electromagnetically coupled and mechanically robust connector to be used in the experimental arrangement. The general format of the database is shown in Fig. 10.

Vector	Input					Output
Parameters	Mag {S11}	Pha {S11}	Re{Zin}	Im{Zin}	VSWR	Status
Array	$X_{Mag\{S11\}}$	$X_{Pha\{S11\}}$	$X_{Re\{Zin\}}$	$X_{Im\{Zin\}}$	X_{VSWR}	Y
Dimension	m x 501	m x 501	m x 501	m x 501	m x 501	m X 1
Type	Real value	Real value	Real value	Real value	Real value	Binary value
Eye bolt 1						Y_1
Eye bolt 2	Data: 501 samples in frequency from 200 MHz to 700					Y_2
...	MHz for each of the 5 parameters.					...
Eye bolt m						Y_m

Fig.10. Structure of the electromagnetic parameters database.

The output of the system is one out of two classes: faulty or faultless, regarding the structural condition of the eye bolts assessed. The minimum threshold that delimits the classes boundaries corresponds to a fault on its initial stage of damage, with length 5.0 mm and depth 0.1 mm.

Additionally, to allow the supervised training of the model, a column vector $Y_{m \times 1} = (y_1,\ y_2, \dots, y_m)^T$ of m binary labels is defined. Each element y_i is the classification label of the bolt corresponding to the ith row of matrix X, being assigned the value 1 if the signal x_i comes from a faulty bolt, and 0, otherwise.

The complete database comprises a total of 2010 elements, being 580 of them from measured bolts and 1430 from simulated bolts. The use of a hybrid database has the advantage of providing a greater number of examples to improve the generalization of the classifier through simulated samples that are easier to obtain. At the same time, the measured samples introduce into the classifier effects that are difficult to obtain by simulation, such as noise, interference, physical imperfections of equipment and materials, as well as variations inherent to the measurement process itself.

The proposed system was designed and trained to detect structural faults in eye bolts of power distribution networks inserted into concrete-made posts, beams, or columns. Although all measured

signals used to build the database have been taken from the same distribution network, once the physical dimensions of the eye bolt under test are the same considered to train the classifier, and it is inserted in a concrete structure, from the point of view of the electromagnetic wave, the propagation medium will be similar to that of the distribution network from which the training samples were obtained. This makes it possible to expand the application of the proposed system for any distribution network, independently of its specific location.

The selection of the random forest as the machine learning model used in the classifier was based on the analysis already presented in [14] that compared 05 different ML algorithms (Logistic Regression, KNN, SVM, Neural Networks and Random Forest) on the detection of faults in anchor rods through the processing of electromagnetic parameters. According to the results presented in [14], the performance of the random forest algorithm outperforms other approaches for the type of application on which the proposed in this work was based.

The random forests algorithm is a supervised learning model that uses the decision tree prediction method, in which each learned parameter is represented by an individual decision tree [33]. The classification of random forest is based on ensemble methods [34], which combine different models to achieve a unique result. Thus, the selection of the final prediction follows the majority voting scheme, meaning that the output chosen by most decision trees becomes the final output of the system [35]. Such a strategy is used to improve the predictive accuracy of the model and avoid overfitting [36].

To evaluate comparatively the performance of the diagnostic system as a function of each electromagnetic parameter used as input, a solution was developed in Python language [37], consisting of a set of independent binary classifiers based on a random forest algorithm composed by 50 decision trees that has been chosen to evaluate the classifier performance [33]-[35]. Such hyperparameters have been chosen to balance both the accuracy and the processing time of the classifier.

Each one of the individual classifiers is independent of the others and receives as input a vector containing the pre-processed samples of one specific electromagnetic parameter. In addition to the individual classifiers associated with each of the 5 parameters assessed, an extra classifier containing the concatenation of all parameters, called an ensemble, was also proposed. Thus, as can be seen in Fig. 11, a total of six distinct classifiers were analyzed.
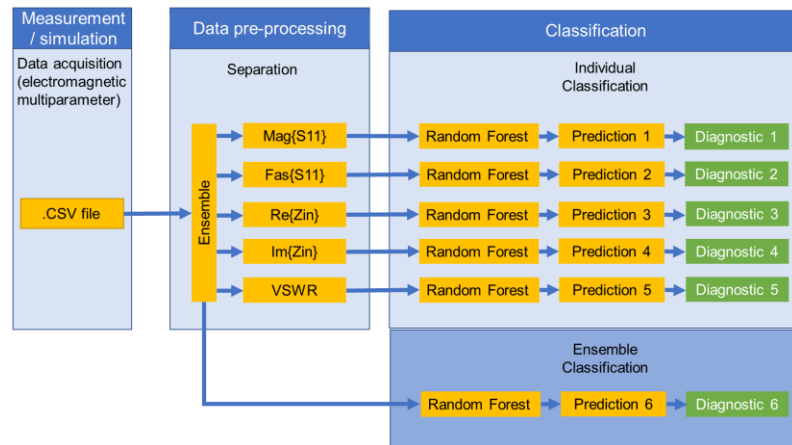
Fig. 11. The architecture of the proposed binary classifier for the evaluation of electromagnetic parameters.

A 10-fold cross-validation method has been used to evaluate the performance of the model in the detection of faults in eye bolts. Such a method consists of randomly splitting the available samples of the database into ten folds, in which, on each iteration, nine of them are used for training and the remaining one is reserved for testing [38]. The overall system performance is calculated using the average of the performances achieved on each iteration.

To analyze and compare the performance of the proposed system with similar approaches available in the literature, the parameters accuracy, precision, recall, and f1-score, will be evaluated. Such parameters are defined in Table IV in the function of the true positives (tp), true negatives (tn), false positives (fp), and false negatives (fn) observed in the predictions performed by the model [4], [38], [39].

Table IV. Definition of performance parameters.

Accuracy	Precision (Prec)	Recall (Rec)	F1-Score
$\dfrac{t_p + t_n}{t_p + t_n + f_p + f_n}$	$\dfrac{t_p}{t_p + f_p}$	$\dfrac{t_p}{t_p + f_n}$	$2 \cdot \dfrac{Prec \cdot Rec}{Prec + Rec}$

V. RESULTS AND ANALYSIS

Taking as a reference the case of the bolt B0 (faultless bolt sample), the Pearson correlation method [40] was applied to evaluate the similarity between the measured and simulated signals for each electromagnetic parameter evaluated, as shown in Table V. It was observed a strong correlation between the measured and simulated signals for all parameters, enabling the use of a hybrid database using both measured and simulated samples to train the machine learning model [41].

Table V. Correlation between the measured and simulated signals for the B0 eye bolt

EM Parameter	Mag.{S11}	Phase {S11}	Im{Z_{in}}	Re{Z_{in}}	VSWR
Pearson Correlation	0.948	0.997	0.992	0.904	0.909

Fig. 12 and 13 shows the comparison between simulated (SIM) and measured results (MEAS) respectively of the five electromagnetic parameters under analysis for two examples of bolts, where one is in the faultless bolt B0, and the other is the faulty sample B5. There are naked-eye observable variations between the normal and defective bolt signals for the five analyzed parameters, making it

possible to differentiate between faultless and faulty bolts. However, it can also be noted that the variations between the signals are subtle and nonobvious. This aspect suggests using a machine learning tool to extract the proper classification features of the signal, and accurately identify the presence or absence of faults in the eye bolt.
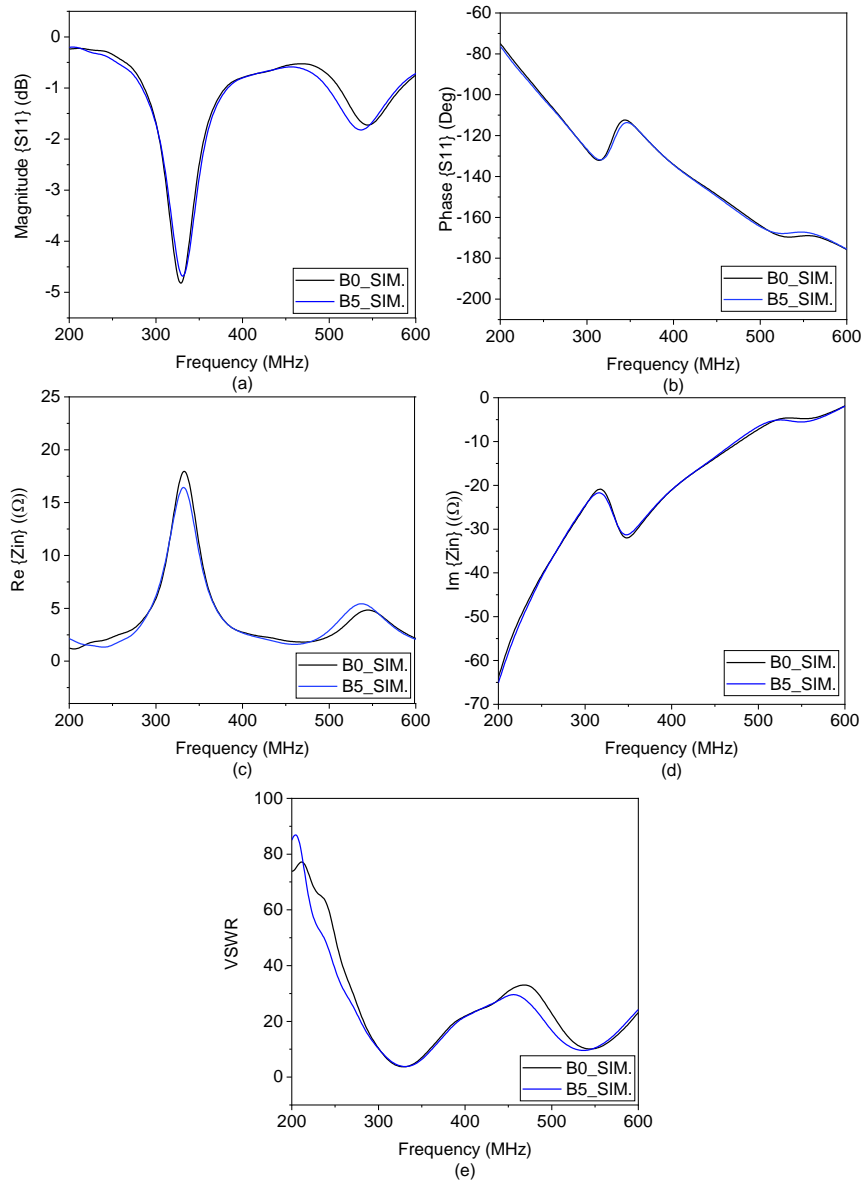

Fig. 12. Comparison of simulated results for eye bolts B0 and B5: (a) Magnitude of S11, b) Phase of S11, c) Real part of Zin, d) Imaginary part of Zin, and e) VSWR.
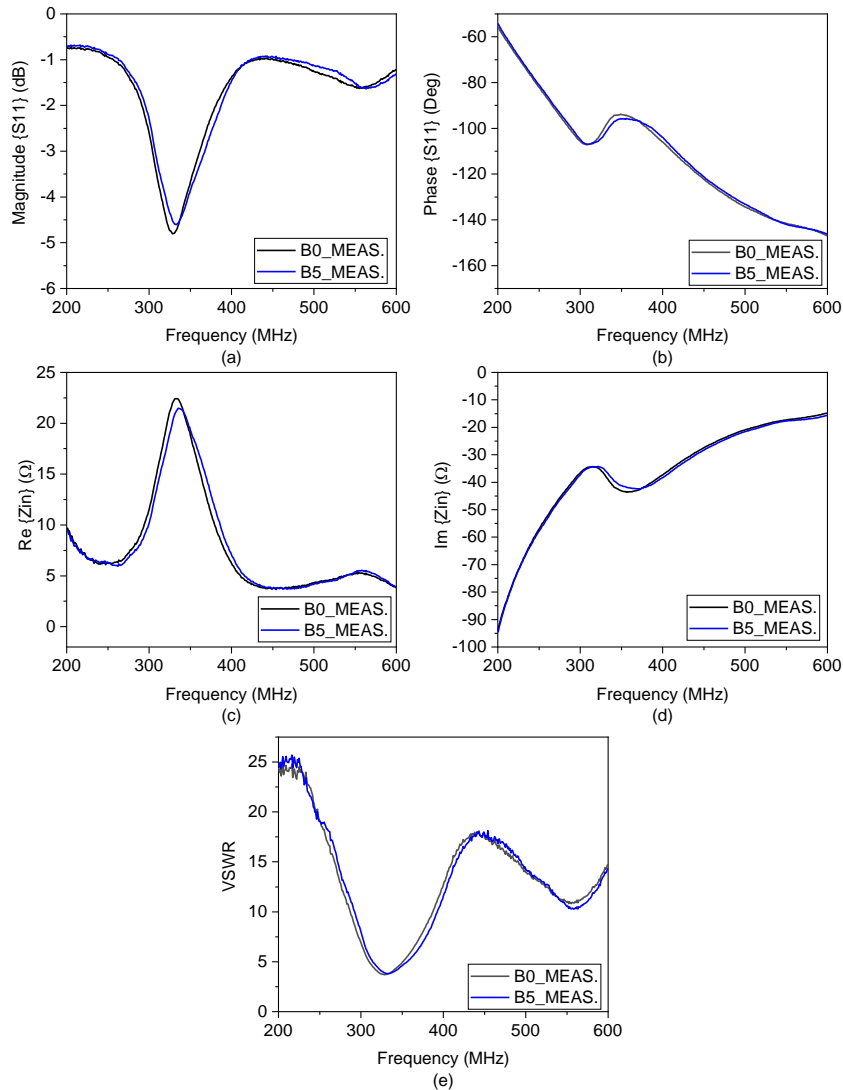
Fig. 13. Comparison of measured results for eye bolts B0 and B5: (a) Magnitude of S11, b) Phase of S11, c) Real part of Zin, d) Imaginary part of Zin, and e) VSWR.

Table VI presents the observed performance of the random forest model for the different electromagnetic parameters, which demonstrates high accuracy, and a good balance between false positives and false negatives in all cases tested.

Table VI. Performance achieved by the random forest model regarding the EM parameters.

Parameters	Accuracy (%)	F1-Score (%)	Rec (%)	Prec (%)
$|S11|$	96.76	98.13	95.08	99.94
Phase {S11}	96.61	97.88	96.53	99.82
VSWR	96.31	98.24	95.97	99.88
Re{Z_{in}}	96.41	97.39	96.08	99.88
Im {Z_{in}}	95.12	97.23	94.13	99.82
Ensemble	97.41	98.36	97.31	99.94

Using a Windows 10 64-bit computer; Processor Intel I5 Dual Core 2.5 GHz; 8 GB RAM, the proposed system took in average only 0.63 s to perform a single detection. Such a relatively fast detection makes it possible to obtain an almost immediate assessment of the integrity of the eye bolts in field measurements through a common laptop. On the other hand, using the same hardware and considering a database composed of 2010 samples of the 5 electromagnetic parameters assessed, the average duration of the training procedure of the random forest classifier was 312 seconds. However, despite this relatively long time, the system is usually required to be trained once. A new training procedure is only performed as a new database is available to upgrade the system.

Fig. 14 presents graphically the accuracy values achieved by the proposed system for each of the 6 parameters analyzed, in addition to 3 baselines of other similar fault detection methods based on machine learning applicable to eye bolt-like structures. The system proposed in [14] achieved an accuracy of 96.14% for the detection of faults in anchor rods of power transmission lines through the analysis of the magnitude of S11 parameter by a random forest algorithm. In [17], an accuracy of 93.33% was obtained in the recognition of anchor rods damage task by a model based on PSO-SVM. The approach presented in [18] obtained an accuracy of 90.11% for an anchor bolt classification based on spectral kurtosis and the K-means clustering algorithm.

It is possible to observe that, for all the parameters except for the imaginary part of Zin, the proposed system achieved values of accuracy superior to the baselines. Comparatively, the ensemble parameter presented the highest accuracy value of 97.41%, and the imaginary part of Zin the lowest, 95.12%. The superior performance of the ensemble model can be explained by the higher amount of information that is provided to the machine learning model by the ensemble data. As the ensemble data is the combination of all the 5 parameters assessed, different representations of the same reflected signal are available to the model, increasing the possibilities of extraction of the set of features that best separates the data from faulty and faultless eyebolts.
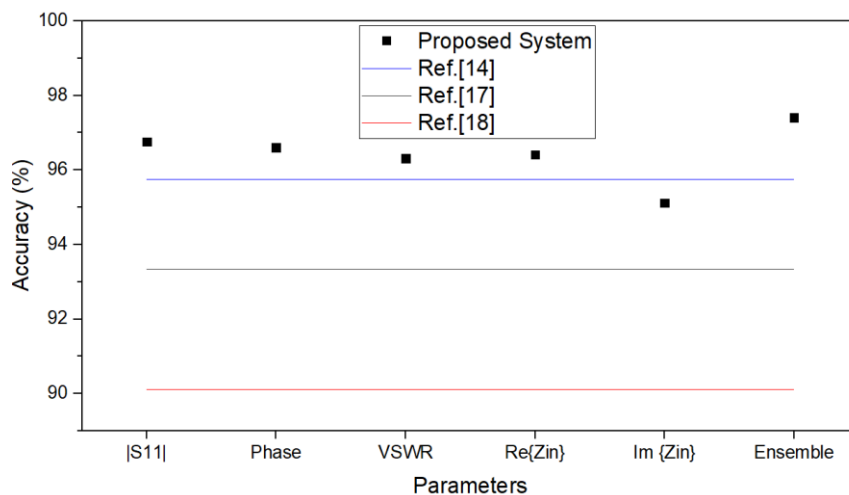

Fig. 14. Comparative performance of the proposed fault detection system.

VI. CONCLUSION

This work proposed a system to noninvasively detect structural faults in eyebolts used for anchoring electrical insulators of substations and power transmission lines. The system is based on the acquisition of multiple electromagnetic parameters related to the reflected high-frequency wave that propagates in the bolt structure. The extraction of features from the signals that allow the identification of normal and faulty bolts is performed automatically by a machine learning algorithm.

The results indicate that using the ensemble database, the random forest model was able to detect structural faults in the bolts with an accuracy of 97.41%. A relatively small misclassification of 2.59% is indeed expected in the system, however, such average error rate is still acceptable for a typical and real field application. With such reliability, it is possible to apply the proposed system to detect the presence of faults in eye bolts safely, without the need dismantling of the anchoring system. This strategy reduces the maintenance costs, the time dedicated to the evaluation of the bolts, and provides a risk reduction in possible financial losses to the power distribution companies.

Future improvements in the system should include the expansion of the database through field measurements, the embedding of the entire system as portable case, and the implementation of an intuitive HMI, to provide the easy acquisition, processing, and analysis of data in the field by maintenance teams. Alternative approaches for fault detection such as the time-domain analysis of the residues of the electromagnetic signals compared to a well-defined pattern of faultless eye bolt response may also be investigated.

REFERENCES

[1] Emad S. Ibrahim, "Corrosion control in electric power systems", *Electric Power Systems Research,* Vol. 52, pp. 9–17, 1999. https://doi.org/10.1016/S0378-7796(98)00133-3.

[2] D. Lauria, S. Minucci, F. Mottola, M. Pagano, C. Petrarca, "Active cathodic protection for HV power cables in undersea application", *Electric Power Systems Research,* Vol 163, pp. 590-598, 2018. https://doi.org/10.1016/j.epsr.2017.11.016.

[3] M. Pompili, B.A. Cauzillo, et al., "Steel reinforced concrete electrodes for HVDC submarine cables", *Electric Power Systems Research,* Vol 163 Part B, pp. 524-531, 2018. https://doi.org/10.1016/j.epsr.2018.05.010.

[4] D. C. P. Barbosa; L. H. A. de Medeiros; M. T. de Melo; L. R. G. S. Lourenço Novo; M. S. Coutinho; M. M. Alves, H. B. D. T. Lott Neto, P. H. R. P. Gama, ; R. G. M. dos Santos and V. L. Tarragô, "Machine Learning Approach to Detect Faults on the Anchor Rods of Power Transmission Lines", *IEEE Antennas and Wireless Propagation Letters,* Vol. 18, pp. 2335–2339, 2019. https://doi.org/10.1109/LAWP.2019.2932052

[5] D. C. P. Barbosa; L. H. A. de Medeiros; M. T. de Melo; L. R. G. S. Lourenço Novo; M. S. Coutinho; M. M. Alves; R. G. M. dos Santos; V. L. Tarragô H. B. D. T. Lott Neto and P. H. R. P. Gama, "An electromagnetic multi-parameter strategy to detect faults in anchor rods using neural networks". 2019 SBMO/IEEE MTT-S International Microwave and Optoelectronics Conference (IMOC), p.3, 2019.

[6] National Electric Energy Agency - ANEEL (Agência Nacional de Energia Elétrica) https://www.aneel.gov.br/, (accessed January 11, 2023).

[7] National Electric Energy Agency – ANEEL Broadcast Services Rules - Electricity, Module 4 Provision of Services. http://www2.aneel.gov.br/cedoc/aren2020906_2_1.pdf, (accessed January 11 04, 2023).

[8] Nicholas Durham , Junhui Zhao , Gregory Bridges and Douglas Thomso, "Acoustic guided wave detection of grounding rod corrosion: equivalent circuit model and implementation". *Smart Materials and Structures,* Vol. 29, p. 55040, 2020. https://doi.org/10.1088/1361-665X/ab72e6.

[9] N. Hirai, Y. Ohki, "Highly sensitive detection of distorted points in a cable by frequency domain reflectometry", Proceedings of 2014 International Symposium on Electrical Insulating Materials, pp. 144–147, 2014. https://doi.org/10.1109/ISEIM.2014.6870741.

[10] Q. Shi, O. Kanoun, "Wire fault diagnosis in the frequency domain by impedancespectroscopy", *IEEE Transactions on Instrumentation and Measurement*, Vol 64, pp. 2178-2187, 2015.https://doi.org/2179–2187. 10.1109/TIM.2014.2386918.

[11] C. Furs, P. Smith, and M. Diamond, "Feasibility of Reflectometry for Nondestructive Evaluation of Prestressed Concrete Anchors", *IEEE Sensors Journal,* Vol. 9, pp. 1322 – 1329, 2009. https://doi.org/10.1109/JSEN.2009.2019309.

[12] Ruslee Sutthaweekul and Gui Y. Tian, Steel Corrosion Stages Characterization Using Open Ended Rectangular Waveguide Probe. *IEEE Sensors Journal,* Vol. 18, pp. 1054 – 1062, 2018. https://doi.org/10.1109/JSEN.2017.2775521.

[13] K. Bouzaffour, B. Lescop, P. Talbot, F. Gallée, and S. Rioual, "Development of an Embedded UHF-RFID Corrosion Sensor for Monitoring Corrosion of Steel in Concrete", *IEEE Sensors Journal*, Vol. 21, pp. 12306-12312, 2021. https://doi.org/10.1109/JSEN.2021.3064970.

[14] Peng Han, Guofu Qiao, Bingbing Guo, "Dongsheng Li and Jinping Ou, Investigation of the low-frequency stray current induced corrosion on reinforced concrete infrastructure in high-speed rail transit power supply system", *Electrical Power and Energy Systems*, Vol. 134, p. 107436, 2022. https://doi.org/10.1016/j.ijepes.2021.107436

[15] L. Novo, M. De Melo, M. De Oliveira, J. Bezerra, L. De Medeiros, R. Aquino, "Design connector for measurements in high frequency on anchor rods", *International Journal of Applied Electromagnetics and Mechanic*, Vol. 45, pp. 457 – 464, 2014. https://doi.org/10.3233/JAE-141864.

[16] M. S. Coutinho, L. R. G. S. Lourenço Novo, M. T. de Melo, L. H. A.de Medeiros, D. C. P. Barbosa, M. M. Alves, V. L. Tarragô, R. G. M. dos Santos, H. B. T. D. Lott Neto and P. H. R. P. Gama, "Machine learning-based system for fault detection on anchor rods of cable-stayed power transmission towers". *Electric Power Systems Research*, Vol. 194, p. 107106, 2021. https://doi.org/10.1016/j.epsr.2021.107106. 347.

[17] H. Zheng, S. Zhang, and X. Sun, "Classification recognition of anchor rod based on PSO-SVM", 29th Chinese Control and Decision Conference (CCDC), pp. 2207-2212, 2017. https://doi.org/10.1109/CCDC.2017.7978881.

[18] Xiao-Yun Sun; Hui Xing; Zhi-Yuan Wang; Ming-Ming Wang and Jian-Pendg Bian, "Classification of anchor bolts based on spectral kurtosis and K-means clustering algorithm", International Conference on Machine Learning and Cybernetics, pp. 93-98, 2016. https://doi.org/10.1109/ICMLC.2016.7860883.

[19] H V H Silva Filho, Marcelo S Coutinho, M T de Melo, E M F de Oliveira, Vinícius L Tarragô, Lauro R G S Lourenco Novo, L M da Silva and Fabio N Fraga, "Design of a connector for fault detection in eye bolts used as insulator anchorages", *Engineering Research Express"*, Vol. 2, p. 45021, 2020. https://doi.org/10.1088/2631-8695/abc9d0.

[20] H. V. H. Silva Filho; D. C. P. Barbosa; M. S. Coutinho; M. T. de Melo, R. G. M. dos Santos, I. Llamas-Garro, "Reliable Structural Failure Detection in Eye Bolts using Reflectometry Signals", 50 th European Microwave Conference (EuMC), pp. 1107-1110, 2021. https://doi.org/10-11.23919/EuMC48046.2021.9338147.

[21] Gao Yongchong, Peng Minfang, Huang Huan, Sun Hongbo and Wu Yuyi, "Design and implementation of intelligent detection equipment for corrosions status of grounding grid", 5 th Asia Conference on Power and Electrical Engineering (ACPEE), pp. 139-143, 2020. https://doi.org/10.1109/ACPEE48638.2020.9136555

[22] M. Fahad; K. Kamal; T. Zafar; R. Qayyum; S. Tariq and K. Khan, "Corrosion Detection in Industrial Pipes Using Guided Acoustics and Radial Basis Function Neural Network", International Conference on Robotics and Automation Sciences (ICRAS), pp. 129-133, 2017. https://doi.org/10.1109/ICRAS.2017.8071930

[23] Feng Pan, "Corrosion detection method of substation Aboveground Steel Structure Based on deep learning", 7th Asia Conference on Power and Electrical Engineering (ACPEE), pp. 2234-2238, 2022. https://doi.org/10.1109/ACPEE53904.2022.9783796

[24] D. C. P. Barbosa; L. H. A. de Medeiros, M. T. de Melo, L. R. G. S. Lourenço Novo, M. S. Coutinho, M. M. Alves, R. G. M. dos Santos, V. L. Tarragô, H. B. D. T. Lott Neto and P. H. R. P. Gama, "Artificial Neural Network-Based System for Location of Structural Faults on Anchor Rods Using Input Impedance Response", *Transactions on magnetics*, Vol. 57, pp. 1-4, 2021. https://doi.org/10.1109/TMAG.2021.3076013

[25] Fangming Deng, Zhongxin Xie, Wei Mao, Bing Li, Yun Shan, Baoquan Wei, Han Zeng, "Research on edge intelligent recognition method oriented to transmission line insulator fault detection", *Electrical Power and Energy Systems*, Vol. 139, p. 108054, 2022. https://doi.org/10.1016/j.ijepes.2022.108054

[26] C. M. Bishop, "Pattern Recognition and Machine Learning", Springer, pp. 124–290, 2006.

[27] V. N. Vapnik, "The Nature of Statistical Learning Theory", Springer, 2nd ed., 1995.

[28] D. M. Pozar, "Microwave engineering", John Wiley & Sons, 4th ed, pp. 48-87 and 165-215, 2011.

[29] D. K. Cheng, "Field and Wave Electromagnetics", Asia: Pearson, 2nd ed., pp. 427-512, 2006.

[30] José M. B. Bezerra; Luiz H. A. de Medeiros; Ronaldo R. B. Aquino; Otoni N. Neto; Lauro R. G. S. L. Novo; Marcos T. de Melo; Daniel S. Santos, Márcio A. B. Fontan, Paulo R. R. Britto, "Localization and Diagnosis of Stay Rod of Guyed Towers Corrosion", 2014 ICHVE International Conference on High Voltage Engineering and Application, pp. 1-5, 2014. https://doi.org/10.1109/ICHVE.2014.7035402.

[31] E. J. P. Santos and L. B. M. Silva, "Calculation of scattering parameters in multiple interface transmission-line transducers", *Measurement*, Vol. 47, pp. 248-254, 2014. https://doi.org/10.1016/j.measurement.2013.08.024

[32] Z. Cendes, "The development of HFSS", 2016 *USNC-URSI Radio Science Meeting*, pp. 39-40, 2016. https://doi.org/10.1109/USNC-URSI.2016.7588501.

[33] L. Breiman, "Random decision forests", *Machine Learning*, Vol. 45, pp. 5–32, 2001. https://doi.org/10.1023/A:1010933404324.

[34] J. Ali et al., "Random forests and decision trees", *International Journal of Computer Science Issues,* Vol. 9, pp. 272–278, 2012.

[35] T. K. Ho, "Random decision forests", Proceedings of 3rd International Conference on Document Analysis and Recognition, Vol.1 pp. 278-282, 1995. https://doi.org/ 10.1109/ICDAR.1995.598994

[36] Fabian Pedregosa, Gael Varoquaux, Alexandre Gramfort, Vincent Michel, Bertrand Thirion, Olivier Grisel, Mathieu Blondel, Peter Prettenhofer, Ron Weiss, Vincent Dubourg, Jake Vanderplas, Alexandre Passos, David Cournapeau, Matthieu Brucher, Matthieu Perrot and ´Edouard Duchesnay, "Scikit-learn: Machine learning in python", *Journal of Machine Learning Research,* Vol. 12, pp. 2825–2830, 2011.

[37] R. Kohavi, "A study of cross-validation and bootstrap for accuracy estimation and model selection", Proceedings of the International Joint Conference on Artificial Intelligence, pp. 1137–1145, 1995.

[38] C. Goutte and E. Gaussier, "A probabilistic interpretation of precision, recall and F-score, with implication for evaluation", European Conference on Information Retrieval, Springer, vol. 3408, pp. 345–359, 2005. https://doi.org/10.1007/978-3-540-31865-1.

[39] Sokolova M., Japkowicz N., Szpakowicz S., "Beyond Accuracy, F-Score and ROC: A Family of Discriminant Measures for Performance Evaluation", Australasian Joint Conference on Artificial Intelligence, Springer, Vol. 4304, pp. 1015-1021, 2006. https://doi.org/10.1007/11941439. https://doi.org/10.1007/978-3-540-31865-1_25

[40] Christian Heumann and Michael Schomaker Shalabh, "Introduction to Statistics and Data Analysis", Springer, 1st ed., pp. 79-90, 2016. https://doi.org/10.1007/978-3-319-46162-5.

[41] Ting Fu, Xiaobo Tang, Zekai Cai, Yu Zuo, Yuming Tang and Xuhui Zhao, "Correlation research of phase angle variation and coating performance by means of Pearson's correlation coefficient", *Progress in Organic Coatings*, Vol. 139, p. 105459, 2020. https://doi.org/10.1016/j.porgcoat.2019.105459.